Please cite this article in press as: Borne and Weiss, Robust spatiotemporal organization of mitotic events in mechanically perturbed *C. elegans* embryos, Biophysical Journal (2024), https://doi.org/10.1016/j.bpj.2024.03.041

Biophysical Journal
Article

Biophysical Society

Robust spatiotemporal organization of mitotic events in mechanically perturbed *C. elegans* embryos

Vincent Borne[1] and Matthias Weiss[1,*]
[1]Experimental Physics I, University of Bayreuth, Universitätsstr. 30, Bayreuth, Germany

ABSTRACT Early embryogenesis of the nematode *Caenorhabditis elegans* progresses in an autonomous fashion within a protective chitin eggshell. Cell-division timing and the subsequent mechanically guided positioning of cells is virtually invariant between individuals, especially before gastrulation. Here, we have challenged this stereotypical developmental program in early stages by mechanically perturbing the embryo without breaking its eggshell. Compressing embryos to about two-thirds of their unperturbed diameter only resulted in markedly slower cell divisions. In contrast, compressing embryos to half of their native diameter frequently resulted in a loss of cytokinesis, yielding a non-natural syncytium that still allowed for multiple divisions of nuclei. Although the orientation of mitotic axes was strongly altered in the syncytium, key features of division timing and spatial arrangement of nuclei remained surprisingly similar to those of unperturbed embryos in the first few division cycles. This suggests that few, very robust mechanisms provide a basic and resilient program for safeguarding the early embryogenesis of *C. elegans*.

SIGNIFICANCE The nematode *Caenorhabditis elegans* features a stereotypical development, with early embryogenesis seemingly running on autopilot. Compressive forces, a potential hazard in the nematode's native habitat, may jeopardize this robust self-organization of the organism. We show that gently compressing embryos only results in markedly slower cell divisions but leaves the early embryonic program otherwise intact. Further compression of embryos impairs cell division, i.e., cell envelopes do not form any longer. However, nuclei still divide in a common cytoplasm ("syncytium") with basic features of division timing and spatial arrangement being remarkably similar to those of unperturbed embryos. This suggests that few robust mechanisms provide a basic program for the early embryonic autopilot.

INTRODUCTION

Embryogenesis is a fundamental and complex process that embraces the emergence of a full-grown multicellular organism from a single cell. Starting from a fertilized oocyte, subsequent cell divisions and the spatial arrangements of these newly formed building blocks into specialized tissues need to be timed and directed without external help. Embryos therefore need to self-organize on many length and time scales and even supposedly simple model organisms such as the nematode *Caenorhabditis elegans* already feature an impressive embryonic self-organization at early stages. In fact, *C. elegans* embryos determine their body axes during the first three rounds of cell divisions, and alongside this they also define precursor cells for distinct tissues, e.g., the germline (1). Moreover, embryos follow a stereotypical development with an invariant cell lineage tree (2) (see Fig. 1 *a* for the first four generations of cells), eventually yielding in 99% of all cases a hermaphroditic adult animal with 959 somatic nuclei.

Given this striking reproducibility, its optical transparency, and the ease with which genetic changes can be induced, *C. elegans* is a widely used model system for studying self-organization during (early) embryogenesis. Combinations of advanced light microscopy and theoretical modeling have revealed, for example, detailed physicochemical insights into the first—asymmetric—cell division (3,4), the onset of cytoplasmic streaming (5–7), and the associated Turing-like pattern formation that supports the definition of germline precursors (8–11). Moreover, chiral force fields have been seen to govern divisions of somatic cells, eventually also determining the animal's left-right

Submitted November 2, 2023, and accepted for publication March 29, 2024.
*Correspondence: matthias.weiss@uni-bayreuth.de
Editor: Chii Jou Chan.
https://doi.org/10.1016/j.bpj.2024.03.041

Please cite this article in press as: Borne and Weiss, Robust spatiotemporal organization of mitotic events in mechanically perturbed *C. elegans* embryos, Biophysical Journal (2024), https://doi.org/10.1016/j.bpj.2024.03.041

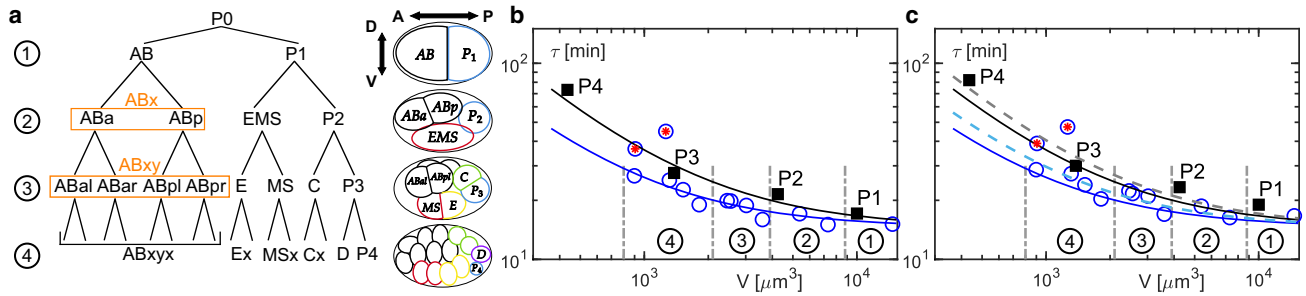

FIGURE 1 (*a*) Lineage tree of the early *C. elegans* embryo with a schematic diagram of cell positions in the respective stages (body axes anterior, posterior, dorsal, and ventral are indicated by *arrows*, and the chitin eggshell is indicated by an *ellipsoidal black line;* adapted from Ref. (1)). Cells of generation 1 (AB, P1) produce daughter cells ABa, ABp, EMS, and P2 (generation 2). Daughter cells of AB are grouped for the analysis (indicated by *orange boxes* with labels $x = a/p$ and $y = l/r$). (*b*) Lifetimes τ, i.e., anaphase to anaphase periods, obtained from unperturbed embryos ($n = 12$) are anti-correlated with cell volumes *V*. Somatic cells (*open blue circles*) and germline cells (*solid black squares*) follow the previously found power-law relation (Eq. 1) (*blue and black lines*, referred to as benchmark curves). Vertical dashed lines and encircled numbers indicate the cell generation (note that P3 and P4 belong to generations 3 and 4, respectively). Cells D and Ea/Ep are highlighted by red asterisks. Note that germline precursors are directly marked here and in Fig. 2. Symbols for individual somatic cells can be identified via the successively smaller volumes in the sequence AB, ABx, EMS, ABxy, MS, E, C, ABxyx, MSx, Cx, Ex, D, ABxyxx. (*c*) Gentle compression of embryos to a diameter of 20 μm ($n = 3$) yielded slightly larger lifetimes (germline, 10%; somatic, 5%–12%) that were still in reasonable agreement with the benchmark curves; same plot style as before. Increasing prefactors α in Eq. 1 by 20%–30% yielded an improved description of the data (*blue and gray dashed lines*). See main text for details. Standard deviations are smaller than symbol size in all cases, i.e., reliable values for cell lifetimes have been obtained even for a low number of gently compressed embryos.

body axis (12,13). In addition, repulsive forces between neighboring cells and/or the engulfing chitin eggshell have been revealed as key determinants for the migration and spatial arrangement of cells until gastrulation (14). Combining this feature with the observation of an inverse relation of cell volume and cell-division times (15–17) suggests that the early embryogenesis of *C. elegans* is an almost deterministic process that virtually runs on autopilot.

Since *C. elegans* embryos seem to "know" how to time cell divisions and to spatially arrange the resulting cellular building blocks in a self-organized fashion, we wondered how these fundamental ingredients for successful embryogenesis would change in response to perturbations. In particular, we asked how robust the timing of mitosis events would be maintained and how space compartmentalization might be altered when driving embryos out of their comfort zone by external cues. Previous data have already revealed that temperature changes within the physiological range only lead to an Arrhenius-like rescaling of division times (17), i.e., in cold conditions the entire development simply progresses more slowly. Only upon exceeding a critical temperature has protein misfolding and degradation been reported to lead to an aberrant development (18). As to aspects of spatial organization, an altered but still optimal cell positioning was observed in very early stages of development when forcing *C. elegans* embryos into pre-defined geometries, from circles to prolate ellipsoids (19). In fact, all observed cell patterns in *C. elegans* embryos and in these artificially constrained geometries are well predicted when modeling cells as soft spheres that mutually interact in a basin with fixed boundary, forcing cells to relax into positions of least mechanical constraints (14,19).

Here we have followed up on these approaches and have explored how a compression of early *C. elegans* embryos, a potential hazard in the native habitat, affects the timing and sequence of mitotic events.

MATERIALS AND METHODS

Embryos from different transgenic *C. elegans* strains were used for this study. In JH2840 (pgl-1:GFP) (20), the p-granule constituent protein PGL-1 is tagged with a green fluorescent protein (GFP); OD95 (GFP::PH(PLC1δ1) + mCherry:his58) (21) features a GFP-labeled plasma membrane and mCherry-labeled histones; XA3051 (GFP::H2B + GFP:tbb-2) (22), a kind gift of I. Mattaj (EMBL), expresses GFP-tagged β-tubulin and histones. Worms were stored and cultured following standard protocols (23). Nematode dissection and egg extraction were performed as described previously (24).

Embryos that are referred to as "unperturbed" were placed in 50-μm- or 120-μm-deep wells (both were seen to not deform the embryo): 50-μm wells were obtained by using double-sided tape as a spacer into which 6-mm-diameter holes were punched. The tape was then glued onto a 24 mm $\times$ 60 mm #1 coverslip (Epredia; Thermo Fisher Scientific, Dreieich, Germany), and single embryos were placed in the hole with a 2-μL droplet of M9 buffer. Holes were sealed by a 20 mm $\times$ 20 mm #1 coverslip (Menzel; Thermo Fisher Scientific) that was placed on top of the tape to avoid evaporation of the medium during the recording. For 120-μm wells, SecureSeal imaging spacer (Grace Bio-Labs, Bend, OR) was used, following the same protocol.

For compressed embryos, polystyrene beads with diameters 20 μm or 12 μm were used as spacers (see Fig. S1, *a–c*). Eggs were placed directly onto #1 coverslips with a droplet of M9 buffer. An additional 2 μL of M9 medium, pre-mixed with a 1% solution of Micromod polystyrene beads (Micromod, Rostock, Germany) was then added and a second coverslip was placed on top, resting on the dispersed polystyrene beads. To avoid movements and medium evaporation, hot Vaseline was carefully applied around the upper coverslip to seal the chamber. Due to bead polydispersity (19.5–20.5 μm and 11.5–13.5 μm, respectively) and since deformed embryos were expected to exert an elastic force against compression, the actual chamber height was controlled by marking both coverslips with a pencil and using the *z*-stage controller to check the distance between these two marks by the focus plane of the confocal microscope. Height control prior to and directly after each time-series acquisition revealed an average sample

Please cite this article in press as: Borne and Weiss, Robust spatiotemporal organization of mitotic events in mechanically perturbed *C. elegans* embryos, Biophysical Journal (2024), https://doi.org/10.1016/j.bpj.2024.03.041

thickness of 20 μm and 14 μm, respectively, without a significant drift between the two times of measurement (Fig. S1 *d*). An unhasty application of the compression allowed embryos to minimize the experienced torque by turning into a position in which the anterior-posterior (AP) axis was parallel to the coverslip. Therefore, all embryos were seen to be compressed perpendicular to the AP axis.

All measurements were performed on a customized spinning-disk confocal microscope, consisting of a Leica DMI 4000 microscope body (Leica Microsystems, Mannheim, Germany) equipped with an SCAN IM 130 × 85 sample stage (Märzhäuser, Wetzlar, Germany), a CSU-X1 (Yokogawa Microsystems, Tokyo, Japan) spinning-disk unit, and a Hamamatsu Orca Flash 4V2.0 sCMOS camera (Hamamatsu Photonics, Hamamatsu City, Japan). The setup was controlled using a custom-made code in LABVIEW (National Instruments, Austin, TX), coupled to the HOKAWO imaging software interface (Hamamatsu Photonics) for image acquisition. Samples were kept at 22.5°C throughout and were imaged with an HC PL APO 63×/1.4 (Leica Microsystems) oil-immersion objective. Illumination of the specimen at 491 nm and 561 nm was achieved by two solid-state lasers (Calypso and Jive; Cobolt, Stockholm, Sweden) in a Dual combiner. The illumination power, measured at the back aperture of the objective, was set to 0.04 mW for 491 nm and to 1.2 mW for 561 nm unless stated otherwise. Fluorescence signals were detected by bandpass filters (Semrock, Rochester, NY) in the range 500–550 nm and 575–625 nm, respectively.

Over a time course of 2–3 h, image stacks of 30 confocal image planes (separated by 1 μm) were acquired every 60 s with 50 ms exposure time for each layer. All embryos were removed from the microscope 2–3 h after the first division, i.e., hatching of fully developed larvae was not monitored but could be anticipated for low laser exposure (13,24–26); embryos exposed to high laser exposure were seen to be dead at this time point. Recording of a single stack required 8–9 s, i.e., a three-dimensional reconstruction of embryos at each instant of their the early development was possible. Image series were analyzed using ImageJ/FIJI with the plugin TrackMate (27) and custom-made codes in MATLAB (The MathWorks, Natick, MA) for tracking nuclei and cell divisions (16); all subsequent analyses were performed with custom-made MATLAB codes.

RESULTS AND DISCUSSION

Aiming to mechanically perturb the seemingly deterministic early development of *C. elegans*, we have exposed individual embryos to compressive forces by sandwiching them between two coverslips (see materials and methods). Since *C. elegans* embryos have an axisymmetric ellipsoidal shape with a long axis of about 50 μm and a diameter of 30 μm, we have used spacings of 50 μm or larger to monitor unperturbed embryos, whereas spacers $\leq$20 μm were used to reduce the diameter of embryos.

As a sensitive readout that reflects on the early developmental program, we have considered the lifetime τ of individual cells (i.e., the period between successive anaphases) along the lineage tree for the first four generations (cf. Fig. 1 *a*). For unperturbed embryos, these lifetimes τ have been shown to display a clear anti-correlation with cell volume V (16,17), i.e.,

$$\tau = \tau_0 + \frac{\alpha}{V} \, . \qquad (1)$$

Here, $\tau_0 \approx 870$ s denotes a cell-independent minimum time that is needed for basic processes such as chromatin (de)condensation. In fact, Eq. 1 is not just an empirical fit to experimental data but can be derived by assuming a limiting factor, e.g., nuclear pore complexes or mitosis-promoting factors, whose copy number per cell is reduced in each cell division (16,17). The parameter α is a constant for somatic and germline cells until gastrulation, but differs about 2-fold between these two lineages ($\alpha_g = 1.86 \times \alpha_s \approx 2.2 \times 10^4$ μm^3/min). No changes were seen when altering the size of embryos via RNAi or when releasing internal mechanical constraints by removing the chitin eggshell (16). Therefore, we will refer to these two lineage-specific relations $\tau(V)$ as "benchmark curves" in the following discussion. Notably, upon varying the ambient temperature in the physiological range, from 15°C to 25°C, all values for τ were seen to change according to a common Arrhenius factor (17), i.e., the developmental program was robust in its timing sequence but with an altered overall timescale (slower development at lower temperatures).

The results summarized in the previous paragraph were revealed with experimental data from light-sheet microscopy, in which *C. elegans* embryos were not subjected to any external mechanical constraints and where illumination-induced phototoxic effects are minimized in comparison to alternative fluorescence imaging techniques (28). Aiming to relate to the benchmark curves, we have probed in a first set of experiments whether confocal imaging of unperturbed *C. elegans* embryos also can yield compatible data for $\tau(V)$. Since confocal imaging at high resolution is gradually compromised in regions that are more distal to the high-numerical-aperture objective (29) (due to a spatially inhomogeneous refraction, absorption, and scattering in the specimen), determining cellular volumes in the 30-μm-thick embryo yielded poor results. We have therefore re-used the previously reported mean cell volumes along the early lineage tree (30) to complement the lifetimes extracted from our confocal imaging approach. As a result, we observed that confocal imaging of unperturbed, i.e., uncompressed, embryos yielded cell lifetimes that were in favorable agreement with the benchmark curves (see Fig. 1 *b*). In the fourth generation, outlier cells D and Ex were seen to deviate from the benchmark curve of somatic cells, featuring significantly larger lifetimes. Such deviations to larger times are actually expected, as these cells are the first in which the cell cycle includes an appreciable gap phase whereas the other cells merely cycle between S- and M-phase (31).

As a next step, we gently compressed embryos to a slightly flattened ellipsoid by using 20-μm spacers for the sandwiching process, i.e., the embryonic diameter was reduced by $\sim$ 10 μm. Such a gentle compression, which leaves the eggshell intact, is widely used as sample-mounting technique for confocal imaging of *C. elegans* embryos (13,24–26) as it reduces the aforementioned limitations on imaging distal regions but allows for live imaging throughout embryogenesis, i.e., the development is not impaired. As a result, we observed that lifetimes in gently

Please cite this article in press as: Borne and Weiss, Robust spatiotemporal organization of mitotic events in mechanically perturbed *C. elegans* embryos, Biophysical Journal (2024), https://doi.org/10.1016/j.bpj.2024.03.041

compressed embryos were still in reasonable agreement with the benchmark curves, although the average values for τ were increased by about 10% (Fig. 1 *c*). One should note the small standard deviation for all measured lifetimes, suggesting that the effect is significant despite the small number of embryos for this condition ($n = 3$). In particular, the lineage-specific relations $\tau(V)$ were preserved, with lifetimes of germline cells being consistently larger than those of somatic cells with comparable volume. In fact, keeping τ_0 in Eq. 1 constant but increasing α_g by 20% and α_s by 30% (*dashed curves* in Fig. 1 *c*) yielded an improved description for the experimental data (as judged from the reduced residuals). Although we cannot extract any quantitative dependence between the level of compression and the values for α, a qualitative explanation for a monotonic increase of α for increasing compression is straightforward: Compression leads, on average, to flattened cells and, therefore, microtubules of the mitotic spindle need to explore larger distances in preparation of a successful cell division. As a consequence, mitosis is slowed down and cell lifetime is increased. In fact, this argument follows earlier explanations for why a failure of cell rounding delays the progress of mitosis in culture cells (32). When preventing cell rounding, the typical distances in the cell are larger than the typical length of microtubules in the mitotic spindle, which delays mitosis because essential spindle checkpoints are not cleared rapidly. Epithelial cells even use the Ras-ERK signaling pathway to adapt to mechanical confinement by updating their shape and mechanical properties, which facilitates cell rounding and proper mitosis (33). Altogether, we can conclude from our data that the timing and sequence of mitotic events in the early development of *C. elegans* is very robust and almost unaffected when applying compressive forces that reduce the embryo to about two-thirds of its native diameter. This goes nicely hand in hand with earlier observations of an unperturbed embryogenesis under such mild confinement (13,24–26).

Interestingly, when challenging embryos with phototoxic stress induced by an approximately 8-fold increased illumination intensity in the blue range (from 0.04 mW to 0.3 mW at 491 nm), we already observed severe changes in the first three generations of cells. For uncompressed embryos, cell lifetimes were on average 30% higher than the benchmark curves (Fig. 2 *a*), and the clear difference between relations $\tau(V)$ for somatic and germline cells was no longer visible. Still, the general anti-correlation of τ and V was preserved. Given that phototoxic stress leads to the emergence of reactive oxygen, the prolonged lifetimes are most likely due to multiple malfunctions that include unspecific protein agglomeration and problems in the respiratory chain. Gently compressed embryos (using again 20-μm spacers that affect at least the natural mode of action of the microtubule cytoskeleton, see above) were seen to be even more sensitive to the illumination-induced phototoxicity, suggesting a synergistic effect of both perturbations. All cell lifetimes were

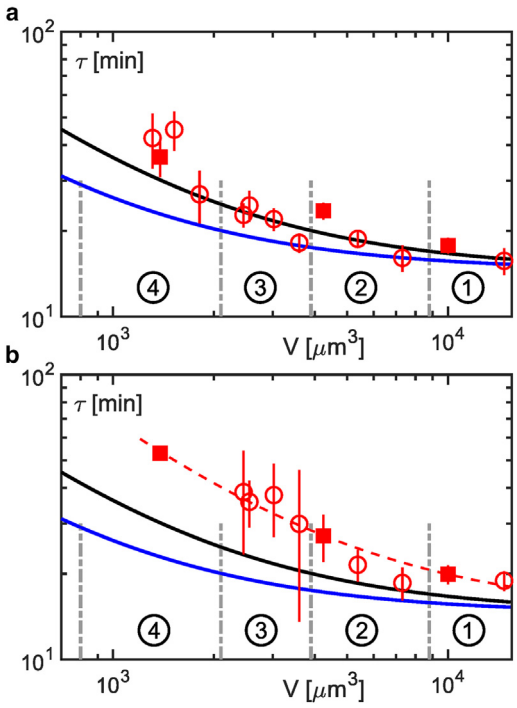

FIGURE 2 Cell lifetimes τ versus volumes V for (*a*) unconstrained embryos ($n = 28$) and (*b*) gently compressed embryos (thickness 20 μm, $n = 7$), when imaged at a markedly increased illumination power in the blue range (0.3 mW at 491 nm). Somatic and germline cells are shown as open circles and filled squares, respectively. In both cases, clear deviations from the benchmark curves (*blue and black lines*) are visible, supposedly due to phototoxic effects that impede proper embryogenesis. Moreover, data sets for somatic and germline cells now overlap, hence perturbing the chronology of cell-division events. Yet, even for the combined challenge of compression and phototoxicity, the general anti-correlation of τ and V according to Eq. 1 is preserved (unaltered τ_0 but $\alpha = 2.5\alpha_g$, *red dashed line*). Error bars (reflecting the standard deviation) are only visible for solid squares when larger than symbol size.

significantly higher than the benchmark curves (on average 57%), and the difference between somatic and germline cells was erased (Fig. 2 *b*). Yet the general anti-correlation of τ and V according to Eq. 1 was maintained and provided (with a strongly increased value for α) a reasonable description of cell lifetimes irrespective of the lineages (cf. *red dashed line* in Fig. 2 *b*). From these data we can conclude that the general scaling (Eq. (1)) is a very robust feature of early *C. elegans* embryos, even when slowly poisoning the (squeezed) organism via phototoxic effects.

As a next step, we increased the mechanical perturbation by using 12-μm spacers to compress *C. elegans* embryos to about half of their native thickness (cf. Fig. S1 *d*). Upon doing so, we frequently observed a total failure of cytokinesis as early as the first cell division (54% of all experiments with these spacers, but 75% of all experiments in which the distance between coverslips was ≤ 15 μm). In particular, in 27 of 36 compressed embryos (diameter ≤ 15 μm) no cytokinesis was observed at all, resulting in a non-natural syncytium state (similar to the syncytial blastoderm of

Please cite this article in press as: Borne and Weiss, Robust spatiotemporal organization of mitotic events in mechanically perturbed *C. elegans* embryos, Biophysical Journal (2024), https://doi.org/10.1016/j.bpj.2024.03.041

Drosophila melanogaster, cf. (34)). In seven cases, the first cytokinesis was successful but subsequent ones were not, yielding two separated syncytia. Only two compressed embryos appeared not to be affected and underwent seemingly normal cytokinesis with asynchronous divisions and timing comparable to that of slightly compressed embryos. In the following we will focus on the vast majority of cases in which a single syncytium emerged, including also a brief discussion on the case of two separated syncytia.

The syncytium state still featured mitotic events and multiple rounds of nucleus duplications (Fig. 3; Videos S1 and S2). This allowed us to define nucleus generations in full analogy to cell generations along the lineage tree in unperturbed embryos (cf. Fig. 1). It is noteworthy that a comparison in terms of nucleus generations for unperturbed and perturbed embryos is actually the most meaningful possibility, since a lack of cytokinesis leads to a constant volume of the syncytium ($\approx 22 \times 10^3\ \mu m^3$), i.e., sorting lifetimes with respect to cell volumes (as done in Figs. 1 and 2) is not possible.

Lifetimes of syncytial nuclei (defined again as the period between successive anaphases) were still seen to increase with every generation, in accordance with cell lifetimes in unperturbed embryos (Fig. 4). This observation suggests that the early developmental program relies on a robust clock that does not require compartmentalization by distinct cells. We did not observe any significant trend between lifetimes and the effective thickness of the squeezed embryo, raising the question as to why lifetime variation was considerably enhanced in the syncytial state. Syncytial nuclei are no longer separated by the plasma membrane of individual cells, i.e., microtubules that are associated with these nuclei (as an aster or as a spindle) have the chance to mutually interact and perturb each other. These interactions most likely can facilitate or delay mitosis, resulting in higher variability of nucleus lifetimes. In accordance with this explanation, we show below that also the mutual distances between syncytial nuclei, supposedly being determined by microtubules, also features a higher degree of variability (cf. Fig. 5 *c*). Moreover, nuclei in the syncytium were seen to always divide in a synchronous fashion. This is in strong

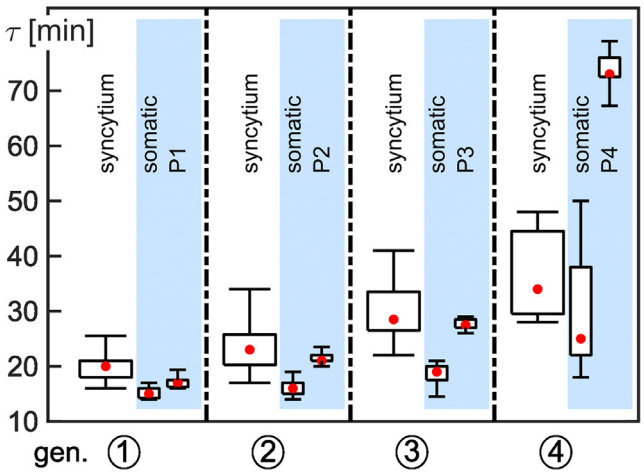

FIGURE 4 Comparison of lifetimes τ of cells/nuclei in unperturbed embryos (*light-blue background*, $n = 12$) and squeezed embryos that have developed a syncytium (*white background*, $n = 27$). The comparison utilizes nucleus generations for ordering, (2^n dividing nuclei in generation n). In generation 1, τ is significantly larger in the syncytium than for the corresponding somatic and germline cells (two-sample Kolmogorov-Smirnov test with threshold $p = 5\%$). In generations 2 and 3, values for τ are significantly larger in the syncytium than in somatic cells but do not significantly differ from germline cells P2 and P3. For generation 4, syncytial nuclei feature an intermediate lifetime between that of somatic and germline cells in unperturbed embryos. Box plots feature the median (*red circle*) and the 25th/75th percentiles (*box*); whiskers represent 1.5 times the interquartile range outside the box.

contrast to unperturbed embryos in which cells divide sequentially, supposedly to ensure proper relaxation of cells to their desired locus (16).

Both observations are in accordance with a previous report. In a pioneering study (35), the chitin eggshell of individual embryos was perforated by laser ablation to allow the uptake of the actin-severing drug cytochalasin D. As a consequence, contractile actomyosin rings were not formed and cytokinesis was suppressed. The resulting syncytium featured synchronous divisions of nuclei, and the division timing appeared to be determined by (unnamed) cytoplasmic factors of all cells that contributed to the syncytium. In particular, division times were seen to be intermediate

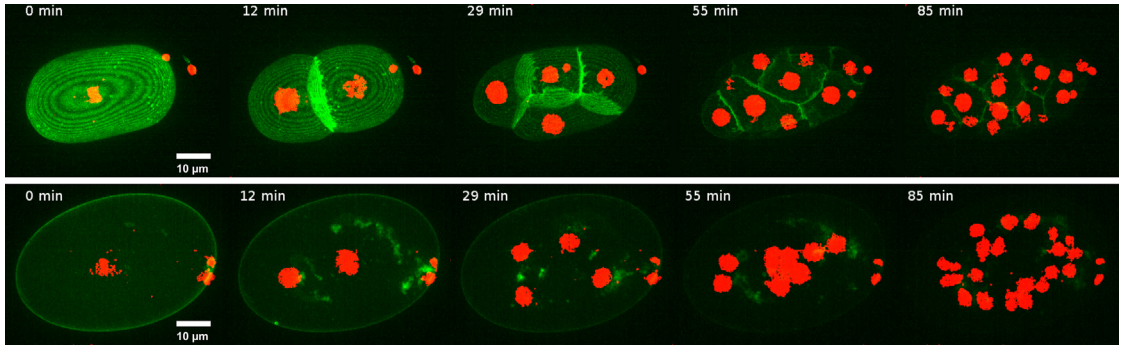

FIGURE 3 Representative fluorescence image series (z-projections) of the development of an unperturbed embryo (*upper panel*) and a strongly squeezed embryo in which cytokinesis fails but nuclei can still divide in a syncytium (*lower panel*). Representative time series for both conditions are available as Videos S1 and S2. Green fluorescence indicates the plasma membrane of cells, while chromatin is highlighted in red.

Please cite this article in press as: Borne and Weiss, Robust spatiotemporal organization of mitotic events in mechanically perturbed *C. elegans* embryos, Biophysical Journal (2024), https://doi.org/10.1016/j.bpj.2024.03.041

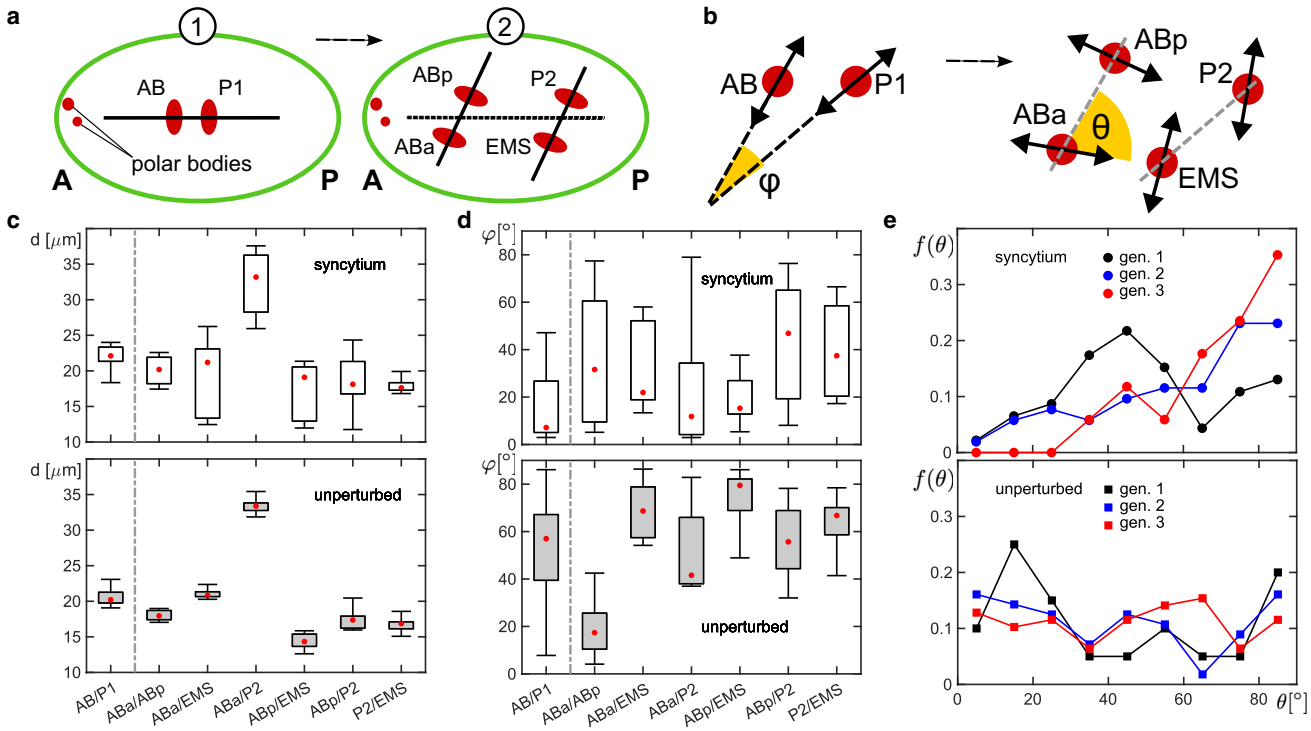

FIGURE 5 (*a*) Sketch of how the AP axis and labels for nuclei were assigned in the syncytium state; see Fig. 1 *a* and the main text for details. (*b*) Definitions of the angle φ between two division axes of nuclei within the same generation and of the angle θ between successive division axes (mother/daughter). (*c* and *d*) Distances d and relative angles of division axes φ for the named pairs of nuclei in the first and second generations. While the distances are very similar in unperturbed embryos (*bottom*) and in the syncytium (*top*), the orientation of division axes is markedly different. (*e*) Probability distribution function of angles between mother and daughter nuclei, $f(\theta)$, with a normalization to relative probabilities (shown as *symbols and lines* instead of histograms for better visibility). Named generations refer to daughter nuclei, i.e., gen. 1 refers to θ values of AB and P1 relative to the AP axis (the division axis of P0). For unperturbed embryos, no clear trend for a preferred angle is visible (except a peak at low angles in the first generation). Successive divisions in the syncytium, however, develop an increasing preference for orthogonal orientations as the generation number increases. See main text for details and discussion. Box plots feature the median (*red circle*) and the 25th/75th percentiles (*box*); whiskers represent 1.5 times the interquartile range outside the box.

between the fastest and the slowest cell that contributed cytoplasm to the syncytium. Even though the formation of a syncytium was enforced biochemically in this case, these earlier observations are fully consistent with our data on mechanically induced syncytia.

A quantitative and generation-wise comparison of nucleus lifetimes further revealed that the timing of mitotic events in the syncytium is quite close to that of germline precursors in the unperturbed embryo (Fig. 4). This observation is somewhat surprising, as one might have expected the syncytium to feature lifetimes that are between those seen for somatic and germline cells. Following up on the idea that cytoplasmic factors eventually determine the timing of mitosis (35), we hypothesize that a component that is present only in germline precursor cells in unperturbed embryos becomes available for all nuclei in the syncytium state, hence synchronizing and shifting cell lifetimes toward values that are typically seen in P cells. Such a cytoplasmic factor might interact or even be a constituent of p-granules, the defining membraneless organelles of germline precursors (36). In unperturbed embryos, p-granules are exclusively observed in P cells, which feature lifetimes that are significantly larger than those of equally sized somatic cells (cf. Fig. 1 *b* and (16)). It is therefore reasonable to assume that p-granules are invoked in prolonging the cell-cycle time, e.g., by sequestering mitosis-promoting factors.

Interestingly, the syncytium state still allows for the assembly and gradient formation of p-granules (see Fig. S2 and Video S3), i.e., p-granules should also able to prolong (and maybe even to synchronize) the cycle time for the division of syncytial nuclei. In fact, p-granules locate initially to the posterior pole of the syncytium (Fig. S2 *c*), similar to what is seen in unperturbed embryos before the first cell division (37). At later stages, p-granules rather assume a perinuclear localization pattern in the syncytium, i.e., p-granules enrich near and around nuclei (Fig. S2 *d* and Video S3), akin to the perinuclear pattern that is seen in P4 cells of unperturbed embryos (36). Based on these observations, one can actually expect the divisions of nuclei in the syncytium to follow the timing of germline precursors for the first generations due to the presence of p-granules near the posterior pole. In the fourth generation, in which the syncytial division timing rather approaches the timing of somatic cells (cf. Fig. 4), the perinuclear

Please cite this article in press as: Borne and Weiss, Robust spatiotemporal organization of mitotic events in mechanically perturbed *C. elegans* embryos, Biophysical Journal (2024), https://doi.org/10.1016/j.bpj.2024.03.041

arrangement of p-granules might not be able to prolong the cell cycle markedly any longer.

At this point, it is also instructive to inspect the behavior of lifetimes in the few cases in which two neighboring syncytia were observed (AB- and P1-syncytium, respectively). During the first and only successful cell division, the vast majority of p-granules is partitioned into the germline precursor P1 (albeit the partitioning might not be as complete as in unperturbed embryos). Therefore, the AB-syncytium can be expected to show lifetimes similar to that of somatic cells, whereas the P1-syncytium should feature larger lifetimes that are near to that of germline precursors in unperturbed embryos. In line with this expectation, lifetimes in the P1-syncytium were always larger than in the AB-syncytium and were in reasonable agreement with values found for P cells (Fig. S3); larger deviations observed in the fourth generation are supposedly due to a gradual enrichment of defects in the squeezed embryo. Lifetimes in the AB-syncytium were consistently higher than those of AB cells in unperturbed embryos, which might be a result of incomplete partitioning of p-granules or other germline-defining components in the first cell division.

Altogether, the observed timing of mitosis events in the non-natural syncytium state is remarkably close to what is seen in unperturbed embryos despite a lack of individual cell envelopes that allow for chemically distinct environments for each nucleus, and hence may support fine-tuning of cell-cycle times.

Going beyond the mere timing, we next asked whether space compartmentalization in the syncytium still follows the cell arrangement observed in unperturbed embryos. Given that cells had been seen to relax into positions of least constraints within the ellipsoidal eggshell (14,16), this would mean that the relative positioning of syncytial nuclei is similar to those of cells in the unperturbed embryo. For a proper comparison between unperturbed and squeezed embryos, we labeled nuclei in the syncytium of compressed embryos in accordance with the corresponding cell names in unperturbed embryos (see schematics in Fig. 1 *a*). To this end, we first defined the AP axis. Since the syncytium retained the ellipsoidal shape of unperturbed embryos, we set the longest axis as the AP axis and defined the anterior pole to be the one in which at least one of the polar bodies remained immobilized (Fig. 5 *a*). This definition is in full analogy to key features of unperturbed embryos (38). Nuclei of the first generation in the syncytium were then identified with the somatic AB cell (anterior) and the germline precursor P1 (posterior) (cf. also Fig. 1 *a*). For the second generation in the syncytium, daughter nuclei of the AB nucleus were labeled as ABa and ABp, depending on whether they were more anterior or posterior (compare Fig. 5 *a* with Fig. 1 *a*). Similarly, the posterior nucleus emerging from division of the P1 nucleus was labeled as P2, and the second daughter nucleus was then named EMS. This assignment of labels becomes more complicated from the third generation onward, since the left-right body axis might be needed to distinguish descendants of nuclei. For simplicity, we have therefore restricted our analysis of the mutual distances of nuclei to the first two generations in which a proper labeling was easily possible.

As a result, we observed that the mutual distances of nuclei in the syncytium follow the cell/nucleus positioning in unperturbed cells (Fig. 5 *c*). In the first generation, the distance between AB and P1 nuclei is basically the same in the syncytium and in unperturbed embryos. In the second generation, stronger fluctuations are observed but the distances are on average still maintained in the syncytium. As mentioned before in the context of lifetimes, the enhanced variability of distances in the syncytium is most likely due to mutual interactions of microtubules that are associated with individual nuclei. The four-cell state of unperturbed embryos, corresponding to the second generation, had been seen to feature a (coplanar) diamond-shaped arrangement of cells/nuclei with the longest distance between ABa and P2 (14), while all other mutual distances were quite similar. This feature is also seen in the syncytium. Therefore, these data suggest that nuclei in the non-natural syncytium state also follow an optimization criterion for their spatial arrangement, namely to assume positions of least mechanical constraints in an ellipsoid, similar to what has been seen before in unperturbed embryos.

Interestingly, the relative angles of division axes, φ, within the first and second generations (see Fig. 5 *b* for a defining sketch) deviate considerably between syncytium and native embryos. In unperturbed embryos, the division axes of AB and P1 enclose an angle of about 45°, whereas the corresponding nuclei in the syncytium divide considerably more collinearly (see Fig. 5 *d*). Similar observations have been made in explants of the syncytial blastoderm of *D. melanogaster* with only two dividing nuclei (34). Therefore, the diamond-shaped arrangement of second-generation nuclei in the syncytium is not already predetermined by the division axes of first-generation nuclei but rather appears to be driven subsequently by repulsive forces, e.g., mediated by microtubule asters that push nuclei to their final positions (34).

Before continuing with the orientation of mitotic axes in the second generation, we would like to discuss the considerable variabilities of φ. These can be explained by a combination of measurement uncertainties and intrinsic fluctuations: To extract the mitotic axis, the center of mass of each chromatin blob in anaphase needed to be determined. This was possible for each blob with an uncertainty of about ± 300 nm. The typical distance between the sister chromatids at the time of quantification was $\approx 5\ \mu$m, yielding an absolute error of about $\pm 2.5°$ for the angle that is enclosed between this mitotic axis and any arbitrary reference axis. The relative angle φ between two mitotic axes is the difference between two of these angles, and therefore has an absolute error of about $\pm 5°$. In addition, the alignment of the active mitotic spindle inside each cell of an unperturbed embryo can be expected to be subject to fluctuations while maintaining a clear preference for a

Please cite this article in press as: Borne and Weiss, Robust spatiotemporal organization of mitotic events in mechanically perturbed *C. elegans* embryos, Biophysical Journal (2024), https://doi.org/10.1016/j.bpj.2024.03.041

certain direction, assuming fluctuations of the orientation of each mitotic axis in the range $\pm 5^\circ$ results in a total variation of $\pm 10^\circ$ in φ due to intrinsic fluctuations. Combining both sources of variation, experimentally determined values φ can be expected to show variations in the range $\pm 15^\circ$, which compares favorably to the 25% and 75% quantiles observed experimentally for unperturbed embryos (Fig. 5 *d*). In the syncytium, intrinsic fluctuations can be expected to be even stronger, e.g., due to mutual interactions of neighboring spindles, which is again in accordance with our experimental observations. Still, the median of φ yields a meaningful measure to compare the gross changes in φ when forcing embryos into the syncytium state.

Relative angles φ between division axes of syncytial nuclei of the second generation also deviate from the unperturbed case. While in unperturbed embryos a small angle between division axes is only seen for ABa and ABp ($\varphi \approx 20^\circ$ instead of $\varphi \approx 60^\circ$ for all other angles), division axes in the syncytium mostly are in the range of small angles ($\varphi \approx 20^\circ$), albeit with very strong fluctuations. These observations suggest that a proper orientation of division axes requires functional cells, i.e., a plasma membrane that can host guiding cues. In particular, self-organizing gradients on, or at, the plasma membrane, e.g., PAR protein gradients (3,4) and/or (chiral) actomyosin force fields (12,13), require an intact cell envelope. The syncytium state may still exploit such guiding cues in the first division, as indicated by the partitioning of p-granules into the posterior part of the embryo (Fig. S2 and Video S3), but in subsequent divisions the lack of interjacent cell envelopes will impede the action of such cues. In other words, without a cell-defining membrane envelope, the spatial arrangement of nuclei can still resemble the unperturbed case in a robust fashion but the well-defined orientations of division axes of unperturbed embryos are basically lost, resulting in a preference for more collinear divisions. Interestingly, the latter finding deviates from the aforementioned explants of syncytial blastoderms of *D. melanogaster* with more than two nuclei, for which a successive randomization of the angle φ has been observed (34). This difference might arise from the fact that nuclei in the syncytium of *C. elegans* embryos are still confined by a rigid eggshell that can provide mechanical cues and boundary conditions, whereas nuclei in explants of the fly embryo are virtually unconfined.

To inspect the geometry of divisions in some more detail, we also extracted the angle enclosed between successive divisions (see sketch in Fig. 5 *b*). In fact, comparing the angle θ between a nucleus division axis in generation n and the division axes of its two daughter nuclei in generation $n+1$ reports on memory effects in successive divisions and whether these necessitate a cell membrane. As a result of our measurements, we observed that nuclei in unperturbed embryos feature a broad range of division angles in each generation with little preference for a particular value of θ (see the distribution of angles in Fig. 5 *e*). Only in the first generation, a distinct peak at small angles is seen that captures the division of P1 preferentially along the AP axis (the division axis of the mother cell P0). From the second generation onward, there is no clear preference for a distinct angle between successive divisions, indicating that selecting division axes is basically devoid of a memory in unperturbed embryos on the level of the whole cell ensemble (individual cells such as P1 or EMS still show a preference for certain angles). In contrast, the syncytium successively develops a clear preference for a 90° angle between successive divisions for increasing generation number on the ensemble level (Fig. 5 *e*). Note that here no assignment of cell labels is necessary, i.e., data beyond the second generation were analyzable for syncytia in a meaningful way as well.

The emerging preference for successive divisions with an orthogonal orientation in the syncytium may be rationalized as follows. During anaphase of a division event, the two centrosomes are located on opposing faces of the newly forming envelopes of the two daughter nuclei. Using the center of mass of the two emerging daughter nuclei as coordinate center, the two centrosome position vectors $\mathbf{r}_1$ and $\mathbf{r}_2$ are, by definition, on the division axis, but point in opposite directions. If the two centrosomes do not move wildly during the following interphase, they will duplicate before the next mitosis event almost at their initial positions, yielding two sister centrosomes per nucleus near to positions $\mathbf{r}_1$ and $\mathbf{r}_2$. Assuming each pair of sister centrosomes to interact in a repulsive manner, e.g., mediated by microtubules that originate from these two organizing centers, the two centrosomes will push each other to a position of largest distance on the (circular) nuclear envelope. Consequently, each of the two sister centrosomes will migrate on the nuclear envelope by an angle of about 90°, eventually resulting in the next division axis to be almost perpendicular to the previous division axis, in line with our experimental observation. Therefore, keeping cells in *C. elegans* embryos intact can be seen as a means to prevent a falling back to the default memory that pushes for orthogonal orientations of the mitotic axes of mother and daughter nuclei.

Altogether, our data show that determining the orientation of division axes appears to be tightly guided by individual cells in unperturbed embryos, hence safeguarding the early development. Although this tuning of division axes is lost in the syncytium, the spatial arrangement of nuclei up to the four-nuclei state is still surprisingly similar to what is seen in unperturbed embryos. Certainly, increasing fluctuations in division angles, as well as the successive mixing of chromatids due to a lack of cell membranes, eventually will disorient the spatial arrangement in the non-natural syncytium of mechanically perturbed *C. elegans* embryos, leading to rapid abort of the development.

CONCLUSION

In summary, we have shown here that gentle compression preserves the timing and sequence of cell divisions in *C. elegans*

Please cite this article in press as: Borne and Weiss, Robust spatiotemporal organization of mitotic events in mechanically perturbed *C. elegans* embryos, Biophysical Journal (2024), https://doi.org/10.1016/j.bpj.2024.03.041

embryos, including a lineage-specific anti-correlation of cell lifetimes and volumes according to Eq. 1. Only upon inducing phototoxic damage, periods between successive divisions were significantly increased and the lineage-specific features were lost, whereas the overall anti-correlation with cell volumes was retained. When compressing embryos to about half of their diameter, cytokinesis was frequently seen to fail, resulting in a non-natural syncytium state that still allows for multiple division cycles of nuclei. The lifetime of syncytial nuclei increases with every generation, in accordance with unperturbed embryos, underlining the robustness of the embryonic timer in early developmental stages. Within the first generations the spatial arrangement of syncytial nuclei is also close to the corresponding cell pattern in unperturbed embryos, suggesting that both are mostly determined by a simple optimization process that favors positions of least mechanical constraints within the ellipsoidal eggshell. In contrast to unperturbed embryos, however, nuclei in the syncytium divided synchronously and displayed altered relative orientations of their division axes, both being reminiscent of observations in the syncytial blastoderm of *D. melanogaster*.

Altogether, our findings suggest that few robust physicochemical cues provide a basic developmental program for timing mitotic events and for guiding the subsequent embryonic compartmentalization, allowing the early development of *C. elegans* to run virtually on autopilot.

SUPPORTING MATERIAL

Supporting material can be found online at https://doi.org/10.1016/j.bpj.2024.03.041.

AUTHOR CONTRIBUTIONS

V.B. performed and analyzed all experiments and contributed to the writing of the manuscript. M.W. designed research, complemented the data analysis, and wrote the manuscript.

ACKNOWLEDGMENTS

Financial support by the DFG (grant WE4335/3-2) and by the Volkswagen-Stiftung (Az. 92738) is gratefully acknowledged. Some strains were provided by the Caenorhabditis Genetics Center funded by the NIH Office of Research Infrastructure Programs (P40 OD010440). We thank Florian Rehfeldt for helpful comments and discussions.

DECLARATION OF INTERESTS

The authors declare no competing interests.

REFERENCES

1. Gonczy, P., and L. S. Rose. 2014. Polarity Establishment, Asymmetric Division and Segregation of Fate Determinants in Early c. elegans Embryos. *WormBook*. 1.
2. Deppe, U., E. Schierenberg, …, G. von Ehrenstein. 1978. Cell lineages of the embryo of the nematode Caenorhabditis elegans. *Proc. Natl. Acad. Sci. USA*. 75:376.
3. Goehring, N. W., P. K. Trong, …, S. W. Grill. 2011. Polarization of par proteins by advective triggering of a pattern-forming system. *Science*. 334:1137–1141.
4. Gross, P., K. V. Kumar, …, S. W. Grill. 2019. Guiding self-organized pattern formation in cell polarity establishment. *Nat. Phys.* 15:293–300.
5. Niwayama, R., K. Shinohara, and A. Kimura. 2011. Hydrodynamic property of the cytoplasm is sufficient to mediate cytoplasmic streaming in the Caenorhabditis elegans embryo. *Proc. Natl. Acad. Sci. USA*. 108:11900–11905.
6. Kimura, K., A. Mamane, …, A. Kimura. 2017. Endoplasmic-reticulum-mediated microtubule alignment governs cytoplasmic streaming. *Nat. Cell Biol.* 19:399–406.
7. Mittasch, M., P. Gross, …, M. Kreysing. 2018. Non-invasive perturbations of intracellular flow reveal physical principles of cell organization. *Nat. Cell Biol.* 20:344–351.
8. Daniels, B. R., E. M. Perkins, …, D. Wirtz. 2009. Asymmetric enrichment of pie-1 in the caenorhabditis elegans zygote mediated by binary counterdiffusion. *J. Cell Biol.* 184:473–479.
9. Daniels, B. R., T. M. Dobrowsky, …, D. Wirtz. 2010. Mex-5 enrichment in the c. elegans early embryo mediated by differential diffusion. *Development*. 137:2579–2585.
10. Han, B., K. R. Antkowiak, …, E. E. Griffin. 2018. Polo-like kinase couples cytoplasmic protein gradients in the c. elegans zygote. *Curr. Biol.* 28:60–69.e8.
11. Wu, Y., B. Han, …, E. E. Griffin. 2018. Rapid diffusion-state switching underlies stable cytoplasmic gradients in the caenorhabditis elegans zygote. *Proc. Natl. Acad. Sci. USA*. 115:E8440–E8449.
12. Naganathan, S. R., S. Fürthauer, …, S. W. Grill. 2014. Active torque generation by the actomyosin cell cortex drives left–right symmetry breaking. *Elife*. 3, e04165.
13. Pimpale, L. G., T. C. Middelkoop, …, S. W. Grill. 2020. Cell lineage-dependent chiral actomyosin flows drive cellular rearrangements in early Caenorhabditis elegans development. *Elife*. 9, e54930.
14. Fickentscher, R., P. Struntz, and M. Weiss. 2013. Mechanical cues in the early embryogenesis of caenorhabditis elegans. *Biophys. J.* 105:1805–1811.
15. Arata, Y., H. Takagi, …, H. Sawa. 2014. Power law relationship between cell cycle duration and cell volume in the early embryonic development of Caenorhabditis elegans. *Front. Physiol.* 5:529.
16. Fickentscher, R., P. Struntz, and M. Weiss. 2016. Setting the clock for fail-safe early embryogenesis. *Phys. Rev. Lett.* 117, 188101.
17. Fickentscher, R., S. W. Krauss, and M. Weiss. 2018. Anti-correlation of cell volumes and cell-cycle times during the embryogenesis of a simple model organism. *New J. Phys.* 20, 113001.
18. Begasse, M. L., M. Leaver, …, A. A. Hyman. 2015. Temperature dependence of cell division timing accounts for a shift in the thermal limits of C. elegans and C. briggsae. *Cell Rep.* 10:647–653.
19. Yamamoto, K., and A. Kimura. 2017. An asymmetric attraction model for the diversity and robustness of cell arrangement in nematodes. *Development*. 144:4437–4449.
20. Gallo, C. M., J. T. Wang, …, G. Seydoux. 2010. Cytoplasmic partitioning of p granule components is not required to specify the germline in c. elegans. *Science*. 330:1685–1689.
21. McNally, K., A. Audhya, …, F. J. McNally. 2006. Katanin controls mitotic and meiotic spindle length. *J. Cell Biol.* 175:881–891.
22. Askjaer, P., V. Galy, …, I. W. Mattaj. 2002. Ran gtpase cycle and importins alpha and beta are essential for spindle formation and nuclear envelope assembly in living caenorhabditis elegans embryos. *Mol. Biol. Cell*. 13:4355–4370.
23. Stiernagle, T. 1999. Maintenance of C. elegans. *In* C. elegans: A Practical Approach. I. Hope, ed Oxford University Press, pp. 51–67.

Please cite this article in press as: Borne and Weiss, Robust spatiotemporal organization of mitotic events in mechanically perturbed *C. elegans* embryos, Biophysical Journal (2024), https://doi.org/10.1016/j.bpj.2024.03.041

24. Bao, Z., and J. I. Murray. 2011. Mounting Caenorhabditis elegans embryos for live imaging of embryogenesis. *Cold Spring Harb. Protoc.* pdb.prot065599.
25. Walston, T., and J. Hardin. 2010. An agar mount for observation of Caenorhabditis elegans embryos. *Cold Spring Harb. Protoc.* pdb.prot5540.
26. Bargmann, C., and L. Avery. 1995. Chapter 10. Laser killing of cells in caenorhabditis elegans. *In* Methods in Cell Biology, Caenorhabditis elegans: Modern Biological Analysis of an Organism, *48*. H. Epstein and D. Shakes, eds. Academic Press, pp. 225–250.
27. Tinevez, J.-Y., N. Perry, …, K. W. Eliceiri. 2017. Trackmate: An open and extensible platform for single-particle tracking. *Methods.* 115:80–90.
28. Keller, P. J., and E. H. K. Stelzer. 2008. Quantitative in vivo imaging of entire embryos with digital scanned laser light sheet fluorescence microscopy. *Curr. Opin. Neurobiol.* 18:624–632.
29. Jonkman, J., C. M. Brown, …, A. J. North. 2020. Tutorial: guidance for quantitative confocal microscopy. *Nat. Protoc.* 15:1585–1611.
30. Fickentscher, R., and M. Weiss. 2017. Physical determinants of asymmetric cell divisions in the early development of caenorhabditis elegans. *Sci. Rep.* 7:9369.
31. Wong, M.-K., V. W. S. Ho, …, Z. Zhao. 2022. Initial characterization of gap phase introduction in every cell cycle of c. elegans embryogenesis. *Front. Cell Dev. Biol.* 10, 978962.
32. Lancaster, O. M., M. Le Berre, …, B. Baum. 2013. Mitotic rounding alters cell geometry to ensure efficient bipolar spindle formation. *Dev. Cell.* 25:270–283.
33. Matthews, H. K., S. Ganguli, …, B. Baum. 2020. Oncogenic signaling alters cell shape and mechanics to facilitate cell division under confinement. *Dev. Cell.* 52:563–573.e3.
34. de Carvalho, J., S. Tlili, …, I. A. Telley. 2022. Aster repulsion drives short-ranged ordering in the Drosophila syncytial blastoderm. *Development.* 149, dev199997.
35. Schierenberg, E., and W. B. Wood. 1985. Control of cell-cycle timing in early embryos of Caenorhabditis elegans. *Dev. Biol.* 107:337–354.
36. Seydoux, G. 2018. The p granules of c. elegans: A genetic model for the study of rna-protein condensates. *J. Mol. Biol.* 430:4702–4710.
37. Brangwynne, C. P., C. R. Eckmann, …, A. A. Hyman. 2009. Germline p granules are liquid droplets that localize by controlled dissolution/condensation. *Science.* 324:1729–1732.
38. Tsai, M. C., and J. Ahringer. 2007. Microtubules are involved in anterior-posterior axis formation in c. elegans embryos. *J. Cell Biol.* 179:397–402.